Enzyme Architecture: The Activating Oxydianion Binding Domain for Orotidine 5′-Monophophate Decarboxylase

Krisztina Spong, Tina L. Amyes, and John P. Richard*

Department of Chemistry, University at Buffalo, SUNY, Buffalo, New York 14260-3000, United States

Ⓢ Supporting Information

ABSTRACT: Orotidine 5′-monophosphate decarboxylase catalyzes the decarboxylation of truncated substrate (1-β-D-erythrofuranosyl)orotic acid to form (1-β-D-erythrofuranosyl)uracil. This enzyme-catalyzed reaction is activated by tetrahedral oxydianions, which bind weakly to unliganded OMPDC and tightly to the enzyme-transition state complex, with the following intrinsic oxydianion binding energies (kcal/mol): SO_3^{2-}, −8.3; HPO_3^{2-}, −7.7; $S_2O_3^{2-}$, −4.6; SO_4^{2-}, −4.5; $HOPO_3^{2-}$, −3.0; $HOAsO_3^{2-}$, no activation detected. We propose that the oxydianion and orotate binding domains of OMPDC perform complementary functions in catalysis of decarboxylation reactions: (1) The orotate binding domain carries out decarboxylation of the orotate ring. (2) The activating oxydianion binding domain has the cryptic function of utilizing binding interactions with tetrahedral inorganic oxydianions to drive an enzyme conformational change that results in the stabilization of transition states at the distant orotate domain.
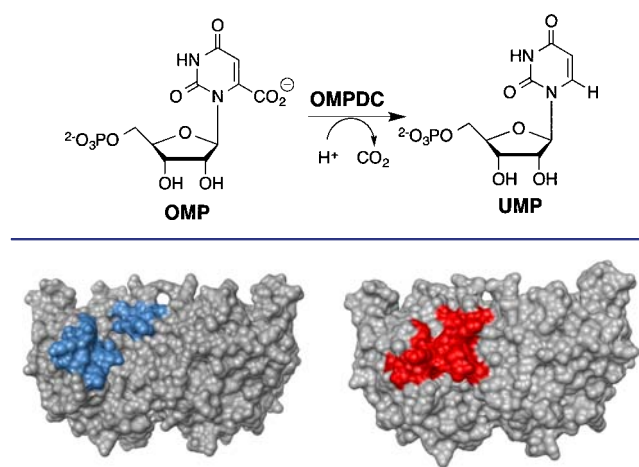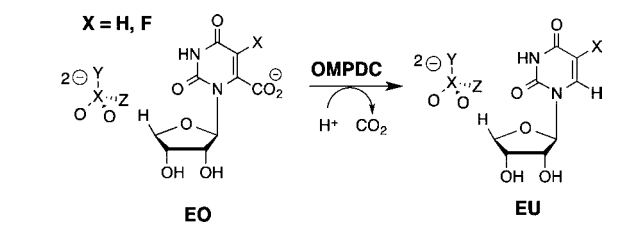
Scheme 1

Figure 1. Space-filling models that show open unliganded ScOMPDC on the left (PDB entry 1DQW), and the complex to 6-hydroxyuridine 5′-phosphate (PDB entry 1DQX) on the right. The colored phosphodianion gripper loop on the left-hand side (Pro202−Val220) and the pyrimidine umbrella (Glu151−Thr165) on the right-hand side of each structure "trap" the ligand at the enzyme active site.

O rotidine 5′-monophosphate decarboxylase (OMPDC) catalyzes the chemically difficult decarboxylation of **OMP** to form uridine 5′-monophosphate (Scheme 1).[1,2] OMPDC provides a startling 31 kcal/mol stabilization of the vinyl carbanion-like transition state for the decarboxylation reaction.[3] By contrast, the observed **OMP** binding energy is 8 kcal/mol,[4] so that the large intrinsic ligand binding energy is only expressed *after* formation of the Michaelis complex to **OMP**.[5,6]

Interactions between the phosphodianion gripper loop (Pro202−Val220) of OMPDC from *Saccharomyces cerevisiae* (*Sc*OMPDC) and the phosphodianion of OMP (Figure 1)[7] result in an 11 kcal/mol stabilization of the transition state for *Sc*OMPDC-catalyzed decarboxylation of the truncated substrate (1-β-D-erythrofuranosyl)orotic acid (**EO**) to form (1-β-D-erythrofuranosyl)uracil (**EU**),[8,9] and a 9 kcal/mol stabilization of the transition state for the catalyzed deuterium exchange reaction of (1-β-D-erythrofuranosyl)-5-fluorouracil (**FEU**, X = F, Scheme 2).[10–12] Phosphite dianion activates OMPDC for catalysis of the decarboxylation and deuterium exchange reactions of these truncated substrates.[8,10] We now report that a series of structurally homologous tetrahedral oxydianions, which includes phosphite dianion, activate OMPDC for catalysis of decarboxylation of **EO**.

The decarboxylation of **EO** catalyzed by *Sc*OMPDC in the presence of tetrahedral inorganic oxydianions (Scheme 2) was

Scheme 2

monitored by HPLC as described in earlier work.[8,13] Figure 2 shows the linear time course that defines the initial velocity (v_i) for the formation of **EU** from the reaction of 5.2 mM **EO** ($\ll K_d$) catalyzed by 5.4 μM *Sc*OMPDC, in the presence of various concentrations of thiosulfate dianion and 10 mM MOPS at pH 7.1 and $I = 0.14$ (NaCl). The values of v_i and the concentration of enzyme and substrate were substituted into eq 1 to give second-order rate constants $(k_{cat}/K_m)_{obs}$ $(M^{-1} s^{-1})$ for

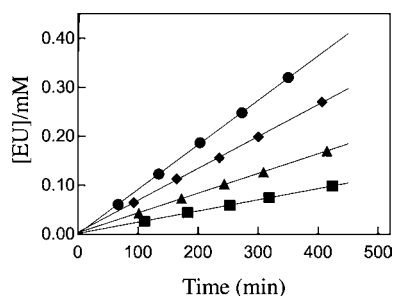$$v_i/[\text{OMPDC}][\textbf{EO}] = (k_{cat}/K_m)_{obs} \qquad (1)$$

Figure 2. Time courses for ScOMPDC-catalyzed decarboxylation of **EO** at pH 7.1, 25 °C, and $I = 0.14$ (NaCl) in the presence of (■) 2.7, (▲) 5.4, (◆) 10.8, and (●) 20.3 mM thiosulfate dianion ($S_2O_3^{2-}$).

the decarboxylation of **EO** by ScOMPDC that are reported in Table S1 (Supporting Information), which also reports the values of $(k_{cat}/K_m)_{obs}$ for the ScOMPDC-catalyzed reactions of **EO** activated by SO_4^{2-} and $HOPO_3^{2-}$ at pH 7.1, 25 °C and $I = 0.14$ (NaCl) determined by the same procedure. There is no detectable activation of the ScOMPDC-catalyzed reactions of **EO** by 33 mM arsenate dianion or 115 mM nitrate anion (Table S1).

The complete time course for the reaction of 0.1 mM **EO** ($\ll K_m$) to give **EU** catalyzed by ScOMPDC in the presence of phosphite (pH 7.0)[8] and sulfite dianion (pH 7.1), buffered by 5 mM MOPS at 25 °C and $I = 0.14$ (NaCl), was monitored spectrophotometrically at 283 nm.[8,9] The reaction in the presence of phosphite dianion exhibited good first-order kinetics for >10 halftimes,[8] but there was a slow downward drift in absorbance for the reaction in the presence of sulfite dianion at >5 reaction halftimes. Control experiments showed that this decrease in absorbance results from reaction of product **EU** with sulfite dianion. The values of k_{obs} (s^{-1}) were determined from the fit of the absorbance data over the first 5 (SO_3^{2-}) or 10 (HPO_3^{2-}) reaction halftimes to a standard single exponential rate equation. These were used to calculate the values of $(k_{cat}/K_m)_{obs} = k_{obs}/[OMPDC]$ reported in Table S1.

Figure 3 shows the dependence of $(k_{cat}/K_m)_{obs}$ for OMPDC-catalyzed reactions of **EO** on the concentration of several oxydianion activators. The solid lines describe the nonlinear least-squares fit of these data to eq 2 derived for Scheme 3,

$$(k_{cat}/K_m)_{obs} = \left(\frac{K_d}{K_d + [X^{2-}]}\right)\left(\frac{k_{cat}}{K_m}\right)_E \\ + \left(\frac{[X^{2-}]}{K_d + [X^{2-}]}\right)\left(\frac{k_{cat}}{K_m}\right)_{E\cdot X} \quad (2)$$

using the previously determined value of $(k_{cat}/K_m)_E = 0.026$ $M^{-1} s^{-1}$[14] and the appropriate values of K_d and $(k_{cat}/K_m)_{E\cdot X}$ from Table 1. The kinetic parameters $(k_{cat}/K_m)_E$, $(k_{cat}/K_m)_{E\cdot X}$ and K_d, for oxydianion activation define three sides of the thermodynamic cycle shown in Scheme 4. Combining the values of $(k_{cat}/K_m)_{E\cdot X}$ and K_d from Table 1 with $(k_{cat}/K_m)_E = 0.026$ $M^{-1} s^{-1}$ (eq 3) for the unactivated decarboxylation

$$K_d^{\ddagger} = \frac{K_d(k_{cat}/K_m)_E}{(k_{cat}/K_m)_{E\cdot X}} \quad (3)$$

reaction gives the values of $K_d^{\ddagger}$ for disassociation of oxydianions from the transition state complex (Table 1).[14]
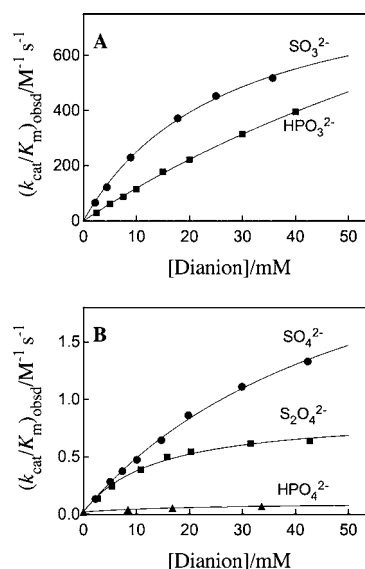

Figure 3. Dependence of second-order rate constants $(k_{cat}/K_m)_{obs}$ for OMPDC-catalyzed turnover of **EO** on the concentration of oxydianion activators.
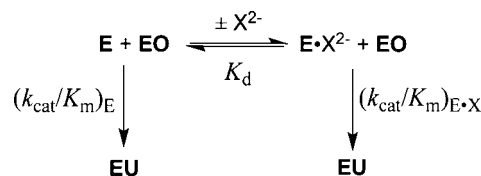
Scheme 3

Table 1. Kinetic Parameters for Activation of OMPDC by Oxydianions and Derived Parameters for Dianion Binding to OMPDC and to $[E\cdot EO]^{\ddagger}$ (Scheme 4)[a]

| oxydianion	K_d, M[b]	$(k_{cat}/K_m)_{E\cdot X}$, $M^{-1} s^{-1}$[b]	$K_d^{\ddagger}$, M[c]	$RT \ln(K_d^{\ddagger})$, kcal/mol[d]
HPO_3^{2-} [e]	0.14	1600	2.3×10^{-6}	−7.7
$HOPO_3^{2-}$	0.025	0.11	5.9×10^{-3}	−3.0
SO_3^{2-}	0.027	920	7.6×10^{-7}	−8.3
SO_4^{2-}	0.055	3.1	4.6×10^{-4}	−4.5
$S_2O_3^{2-}$	0.014	0.87	4.2×10^{-4}	−4.6
$HOAsO_3^{2-}$		no detectable activation		

[a]For reactions at pH 7.1, 25 °C, and $I = 0.14$ (NaCl) unless noted otherwise. [b]Experimental kinetic parameter defined by Scheme 3. [c]Disassociation constant for release of the oxydianion from the transition state complex, calculation using eq 3 derived for Scheme 4. [d]The intrinsic dianion binding energy. [e]Reactions at pH 7.0 (ref 8).

Scheme 4
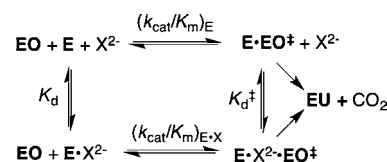
The binding energies $\Delta G^{\ddagger}$ for formation of different complexes $[E\cdot X^{2-}\cdot EO]^{\ddagger}$, calculated from $K_d^{\ddagger}$, are reported in Table 1 and Chart 1. We conclude that these dianions are powerful activators of OMPDC-catalyzed decarboxylation, and that this activity for activation has been recruited for **OMP** by tethering the phosphodianion to the nucleoside orotidine.

Chart 1

$$\Delta G^{\ddagger} \text{ kcal/mol} \quad -8.3 \quad -7.7 \quad -4.6 \quad -4.5 \quad -3.0 \quad \approx 0$$
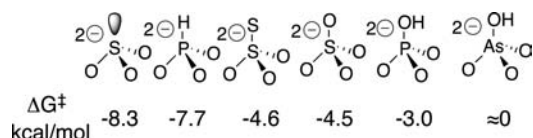
Free OMPDC shows a weak affinity for tetrahedral oxydianions ($K_d \geq 0.027$ M), and the $[\text{E·EO}]^{\ddagger}$ complex (Scheme 4) shows a high affinity for binding oxydianions. This complex has the largest affinity (8 kcal/mol) for isoelectronic HPO_3^{2-} and SO_3^{2-}. The increase in dianion size and reduction in charge density at the individual oxygen of SO_4^{2-} compared with SO_3^{2-} result in a decrease in the intrinsic dianion binding energy from -8.3 to -4.5 kcal/mol. The similar -4.5 and -4.6 kcal/mol intrinsic binding energies for SO_4^{2-} and $S_2O_3^{2-}$, respectively, may reflect the offsetting effects of the larger size of the -S^{-} at $S_2O_3^{2-}$ compared with -O^{-} at SO_4^{2-}, and the greater charge at the electronegative oxygen atoms of $S_2O_3^{2-}$ that interact with protein side chains. The small -3.0 kcal/mol intrinsic dianion binding energy for $HOPO_3^{2-}$ and the >8 kcal/mol difference between the dianion binding energies for HPO_3^{2-} and $HOAsO_3^{2-}$ are consistent with demanding steric/polar requirements to obtain the precise fit at the dianion binding site required for optimal enzyme activation. The reproduction of these intrinsic dianion binding energies provides a stringent test for computational methods developed to model catalysis by OMPDC.[15−17]

The X-ray crystal structure of the complex between yeast OMPDC and the intermediate analogue 6-hydroxyuridine 5′-phosphate (**BMP**, Figure 4) reveals interactions between the
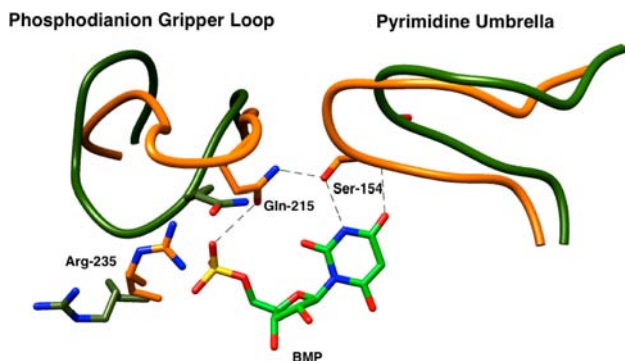

Figure 4. X-ray crystal structure (PDB entry 1DQX) of yeast OMPDC in a complex with 6-hydroxyuridine 5′-phosphate that shows interactions of the phosphodianion with the side chains from a loop that runs from Pro202 to Val220 and of the pyrimidine ring with a hydrophobic umbrella that runs from Ala151 to Thr165. The connecting hydrogen bond is between the side chains of Gln215 and Ser154. Reprinted with permission from ref 18. Copyright 2013 American Chemical Society.

ligand phosphodianion and the polar side chains of Gln215 and Tyr217 (not drawn in Figure 4) in the phosphodianion gripper loop (Pro202−Val220) and with Arg235. The orotate ring interacts with residues from a hydrophobic umbrella (Ala151−Thr165). The *gripper* loop is well separated from the site of decarboxylation. For example, the distance between the guanidinium nitrogen and the C-6 oxygen of **BMP** is ca. 10 Å. The Q215A, Y217A, and R235A mutations at OMPDC have little (≤2.4-fold) effect on k_{cat}/K_m for decarboxylation of the

phosphodianion truncated substrate **EO**, so that there are no more than weak interactions between these side chains and the transition state for decarboxylation at the distant pyrimidine ring.[14] By contrast, the Q215A, Y217A, and R235A mutations result in up to 10^4-fold decreases in k_{cat}/K_m for catalysis of decarboxylation of **OMP** and in $(k_{cat}/K_m)_{E·X}/K_d$ (Scheme 4) for dianion activation of the catalyzed decarboxylation reaction of **EO**, so that these enzyme-dianion interactions are utilized in the stabilization of transition states that form at the distant catalytic site.[14,18]

The strong dependence of the magnitude of enzyme activation on the oxydianion structure (Table 1) demands a precisely *structured* enzyme active site in order to obtain the extraordinary rate acceleration observed for OMPDC. The results may be rationalized by a model where the unactivated $((k_{cat}/K_m)_E$, Scheme 4) and dianion activated $((k_{cat}/K_m)_{E·X})$ decarboxylation reactions proceed through a single high-energy, catalytically active, loop-closed form of OMPDC that is stabilized by hydrogen bonding and ion-pairing interactions between dianions and the gripper loop.[6,19−21] We cannot rigorously exclude the possibility that the two decarboxylation reactions are catalyzed by different conformations of OMPDC. However, the reactive enzyme conformation must form at some low concentration in the absence of added dianions, so that the utilization of a single protein conformation to catalyze both reactions provides for the greatest economy in reaction pathways. An important element of the enzyme conformational change is formation of a hydrogen bond between the side chains of Ser154 and Gln215 (Figure 4).[13] This couples closure of the gripper loop, which alone is not expected to strongly activate OMPDC for decarboxylation at the distant catalytic site, and closure of the pyrimidine umbrella, which we propose strongly activates OMPDC for catalysis of decarboxylation of **OMP** or **EO**.[18]

Wolfenden proposed that optimal enzymatic catalysis of many reactions is best obtained at an active site where the substrate is trapped in a protein cage (Figure 1) and completely surrounded by functional groups of the enzyme.[22] We propose for OMPDC that the exclusive catalytic role of protein−dianion interactions is the stabilization of this active closed protein cage (Figure 1), and that transfer of **OMP** from water to the protein cage is energetically uphill for the reaction of **EO** and assisted by interactions between OMPDC and the phosphodianion of **OMP**. The precise conformational changes associated with formation of caged enzyme−substrate complexes are expected to differ for enzymes that utilize the intrinsic dianion binding energy to stabilize the transition states for decarboxylation (OMPDC),[8] proton transfer (triosephosphate isomerase, TIM),[23] hydride transfer (glycerol 3-phosphate dehydrogenase),[24] phosphoryl transfer (phosphoglucomutate),[25] reducto-isomerization (1-deoxy-D-xylulose 5-phosphate reductoisomerase)[26] and, almost certainly, other enzymatic reactions. However, these mechanistic issues have not been probed in detail, except for recent mutagenesis studies on the isomerization reaction catalyzed by TIM.[27−30]

■ ASSOCIATED CONTENT

Ⓢ Supporting Information

Table S1, kinetic parameters for turnover of EO by OMPDC in the presence of oxydianions at pH 7.1 and $I = 0.14$ maintained with NaCl. This material is available free of charge via the Internet at http://pubs.acs.org.

■ AUTHOR INFORMATION

Corresponding Author
jrichard@buffalo.edu

Notes
The authors declare no competing financial interest.

■ REFERENCES

(1) Miller, B. G. *Top. Curr. Chem.* **2004**, *238*, 43−62.

(2) Miller, B. G.; Wolfenden, R. *Annu. Rev. Biochem.* **2002**, *71*, 847−885.

(3) Radzicka, A.; Wolfenden, R. *Science* **1995**, *267*, 90−93.

(4) Porter, D. J. T.; Short, S. A. *Biochemistry* **2000**, *39*, 11788−11800.

(5) Jencks, W. P. *Adv. Enzymol. Relat. Areas Mol. Biol.* **1975**, *43*, 219−410.

(6) Amyes, T. L.; Richard, J. P. *Biochemistry* **2013**, *52*, 2021−2035.

(7) Miller, B. G.; Hassell, A. M.; Wolfenden, R.; Milburn, M. V.; Short, S. A. *Proc. Natl. Acad. Sci. U.S.A.* **2000**, *97*, 2011−2016.

(8) Amyes, T. L.; Richard, J. P.; Tait, J. J. *J. Am. Chem. Soc.* **2005**, *127*, 15708−15709.

(9) Toth, K.; Amyes, T. L.; Wood, B. M.; Chan, K. K.; Gerlt, J. A.; Richard, J. P. *Biochemistry* **2009**, *48*, 8006−8013.

(10) Goryanova, B.; Amyes, T. L.; Gerlt, J. A.; Richard, J. P. *J. Am. Chem. Soc.* **2011**, *133*, 6545−6548.

(11) Tsang, W.-Y.; Wood, B. M.; Wong, F. M.; Wu, W.; Gerlt, J. A.; Amyes, T. L.; Richard, J. P. *J. Am. Chem. Soc.* **2012**, *134*, 14580−14594.

(12) Amyes, T. L.; Wood, B. M.; Chan, K.; Gerlt, J. A.; Richard, J. P. *J. Am. Chem. Soc.* **2008**, *130*, 1574−1575.

(13) Barnett, S. A.; Amyes, T. L.; Wood, B. M.; Gerlt, J. A.; Richard, J. P. *Biochemistry* **2008**, *47*, 7785−7787.

(14) Amyes, T. L.; Ming, S. A.; Goldman, L. M.; Wood, B. M.; Desai, B. J.; Gerlt, J. A.; Richard, J. P. *Biochemistry* **2012**, *51*, 4630−4632.

(15) Gao, J. *Curr. Opin. Struct. Biol.* **2003**, *13*, 184−192.

(16) Warshel, A.; Florian, J.; Strajbl, M.; Villa, J. *ChemBioChem* **2001**, *2*, 109−111.

(17) Vardi-Kilshtain, A.; Doron, D.; Major, D. T. *Biochemistry* **2013**, *52*, 4382−4390.

(18) Goryanova, B.; Goldman, L. M.; Amyes, T. L.; Gerlt, J. A.; Richard, J. P. *Biochemistry* **2013**, *52*, 7500−7511.

(19) Richard, J. P. *Biochemistry* **2012**, *51*, 2652−2661.

(20) Go, M. K.; Amyes, T. L.; Richard, J. P. *Biochemistry* **2009**, *48*, 5769−5778.

(21) Malabanan, M. M.; Amyes, T. L.; Richard, J. P. *Curr. Opin. Struct. Biol.* **2010**, *20*, 702−710.

(22) Wolfenden, R. *Mol. Cell. Biochem.* **1974**, *3*, 207−211.

(23) Amyes, T. L.; Richard, J. P. *Biochemistry* **2007**, *46*, 5841−5854.

(24) Tsang, W.-Y.; Amyes, T. L.; Richard, J. P. *Biochemistry* **2008**, *47*, 4575−4582.

(25) Ray, W. J., Jr.; Long, J. W.; Owens, J. D. *Biochemistry* **1976**, *15*, 4006−4017.

(26) Kholodar, S. A.; Murkin, A. S. *Biochemistry* **2013**, *52*, 2302−2308.

(27) Zhai, X.; Amyes, T. L.; Wierenga, R. K.; Loria, J. P.; Richard, J. P. *Biochemistry* **2013**, *52*, 5928−5940.

(28) Malabanan, M. M.; Nitsch-Velasquez, L.; Amyes, T. L.; Richard, J. P. *J. Am. Chem. Soc.* **2013**, *135*, 5978−5981.

(29) Malabanan, M. M.; Koudelka, A. P.; Amyes, T. L.; Richard, J. P. *J. Am. Chem. Soc.* **2012**, *134*, 10286−10298.

(30) Malabanan, M. M.; Amyes, T. L.; Richard, J. P. *J. Am. Chem. Soc.* **2011**, *133*, 16428−16431.